Research Paper

Journal of JSAM 85(3) : 1～10, 2023

Detection of Target Reference Points of a Hand Tractor Based on Transfer Path Analysis Technique

Sovatna PHON*1, Eiji INOUE*2, Muneshi MITSUOKA*3†,
Takashi OKAYASU*2, Yasumaru HIRAI*2

Abstract

In this study, transfer path analysis (TPA) technique was employed to estimate the best reference points to the response point of a hand tractor. Six locations of the hand tractor, specifically, engine-right-side front, engine-right-side rear, engine-cover top, chassis, gearbox, and middle between handle-base and handgrip were considered as reference points; whereas, handgrip was regarded as a response point. For TPA analysis, the power spectrum densities of the seven locations were populated into a 3rd-order tensor. To improve the accuracy of response point vibration estimation, two reference points were selected for TPA analysis. Finally, the best contribution was determined using the root mean square error (RMSE) methods. Result indicated that chassis-gearbox combination are the best target points for the response point.

[Keywords] transfer path analysis, vibration characteristics, hand tractor, reference points, target points

I Introduction

The adoption of hand tractors as substitutes for human workers and draft animals has become an extremely significant matter for field operations in Cambodia. The hand tractor not only facilitates the timely completion of operations but also increases production, labor savings, energy efficiency, productivity, and profitability (Singh et al., 2011). In addition, the hand tractor is suited to the sizes and scattered locations of farms, can be used in dry and wet conditions, has low cost, and multiple uses (Chan, 2013; FAO, 2013).

Numerous applications of hand tractors have resulted in workers holding handles for longer, resulting in early fatigue caused by vibrational discomfort. Tiwari et al. (2006) explained that machine vibrations are detrimental to agricultural workers. Many studies have confirmed the adverse health effects of vibration. For example, early fatigue may cause physical, physiological, and musculoskeletal disorders over months and years (Salokhe et al., 1995; Sam et al., 2006; Dewangan et al., 2009).

Vibration signals are produced in a complex form; therefore, to achieve a comfortable condition, it is essential to reduce the interior vibration at the handle of the hand tractor. During this process, sensors should be installed at desirable reference locations to obtain vibrational behaviors at the response point of the hand tractor to minimize the number of vibration sensor allocation uses (Yoshida et al., 2013).

To visualize the contribution of a range of different factors to vibration levels and effectively measure the interior vibrations of the hand tractor, an ideal method to determine the effective locations for vibration reduction, the transfer path analysis (TPA), was developed. The transmitted vibration from an engine overlap in a complex manner with various noises or vibrations; therefore, the transfer path analysis has proved to be an effective method (Nomura and Yoshida, 2006; Nomura, 2011).

TPA can also be applied to characterize the sensitivity effect caused by noise and the strong relationship between the input signals of a control system and output signals; thus, in addition to performing contribution

*1 JSAM Member, Pursat Provincial Department of Agriculture, Forestry and Fisheries, Peal Nhek II Village, Sangkat Ptah Prey, Pursat City, Pursat Province, Cambodia
*2 JSAM Member, Faculty of Agriculture, Kyushu University, 7–4–4 Motooka, Nishi-ku, Fukuoka 819–0395, Japan
*3 JSAM Member, Faculty of Agriculture, University of Ryukyus, 1 Senbaru, Nishihara, Okinawa 903–0213, Japan
† Corresponding author : mitsuoka@agr.u-ryukyu.ac.jp

separation, it has been used to set the reference signal targets and suggest countermeasure guidelines (Cowell, 1969; Erdal et al., 2013).

To implement the TPA, in this experiment, power spectral densities (PSDs), which were obtained from a calculation of time-series signals using the fast Fourier transform (FFT) technique at reference points and response points, were applied. This TPA method is a useful analytical tool for determining the main contributions to vibration in hand tractors and for developing effective countermeasures to maintain vibrations below the target levels. Therefore, in the present study, "reference points to the response point through vibration transmission using transfer path analysis" were studied to determine the best reference point location where it represents the vibration characteristics at the handgrip using transfer path analysis method (TPA). Furthermore, this reference point can be regarded as the site that contributes significantly to the vibration transmission from the vibration source to the handgrip (response point). Therefore, vibration countermeasures at the selected reference point contribute to vibration reduction at the handgrip (response point).

II Materials and methods

1. Experimental setup

A diesel hand tractor was used for the experiment under dynamic conditions on an asphalt road, as shown in Fig. 1. The specifications of the hand tractor are listed in Table 1. Typically, a hand tractor is not designed to be equipped with an engine speed gauge; therefore, we measured the rotational speed of the shaft, reduced by the belt, using a laser tachometer at five engine throttle opening revels instead of the engine speed.

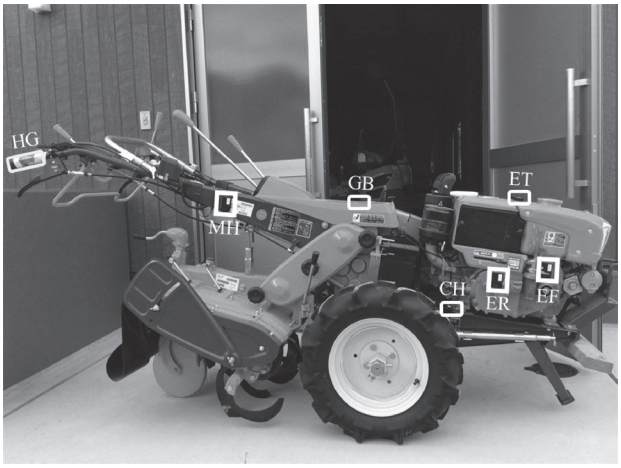

Fig. 1 Experimental hand tractor and sensor allocations

Table 1 Specifications of the experimental hand tractor

Specification	
Length (mm)	2210
Width (at handles) (mm)	720
Height (mm)	1250
Weight (kg)	288
Cooling system	Horizontal water-cooled fan
Output (kW)	5.5
Rated speed (rpm)	2500
Implement width (mm)	600
Implement diameter (mm)	400

Five engine throttles were picked up at 650, 880, 1050, 1200, and 1300 revolution per minute (rpm), where 650 rpm was the lowest engine throttle, and 1300 rpm was the highest engine throttle by using a laser tachometer.

2. Sensor arrangement

Seven wireless sensors (Sports Sensing, SS-MS-SMA5G3) were firmly taped at different points on the hand tractor: the engine-right-side front (EF), engine-right-side rear (ER), engine-cover top (ET), chassis (CH), gearbox (GB), middle between handle base and handgrip (MH), and handgrip (HG), as shown in Fig. 1. The locations of the six reference points, except for handgrip, were determined by the ease of sensor installation, rigidity, and proximity to vibration sources such as vibration from the engine or road surface. Fig. 2 presents a sensor feature, and the specifications of the sensor are shown in Table 2. The performances of the sensors were recorded in 6 degrees of freedom such as 3-translational acceleration data, 3-rotational angular

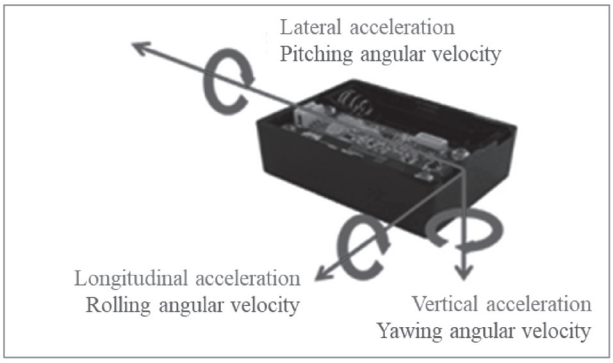

Fig. 2 About wireless sensor

Table 2 Specification of DSP analog voltage data logger

Specification	
Name of sensor	SS-MS-HMA5G3
Translational acceleration range	±5 G
Angular velocity range	±300 dps
Sampling rate	1 H～1000 Hz (9 degrees of freedom)
Resolution	16 bit

velocity data at a sampling rate of 200 Hz. The data are instantly stored in memory and backed up on the computer through wireless communication using a DSP(Digital Signal Processor) analog voltage data logger (Sports Sensing, SS-RF24TR1).

3. Feature extraction and analysis methods

3. 1 Processing technique

The instant data in the memory of the sensors were backed up on a computer, manipulated, and analyzed using the open-source programming language, Python 3.7.4, and its libraries; numpy 1.18.1, pandas 1.0.2, matplotlib 3.1.3, scipy 0.16.2 and sklearn 0.16.2 under the Anaconda 4.12.0, Jupyter Notebook 6.0.3. It provides powerful tools to calculate the RMS value, FFT, PSD, dominant frequency of measured time series, singular value decomposition (SVD), TPA technique, inverse time series from FFT. The data analysis process is illustrated in Fig. 3.

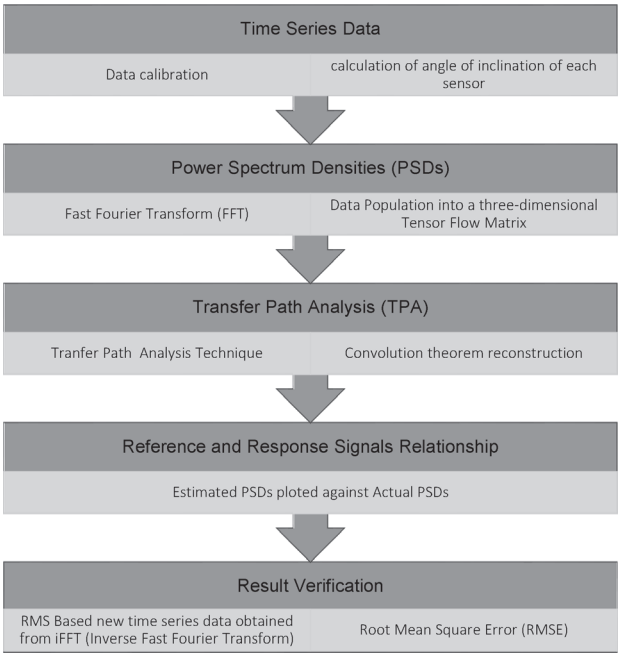

Fig. 3 Block-diagram for feature extraction and analysis

3. 2 Feature extraction for TPA technique

In principle, few steps are followed for data or feature extraction. First, in a dynamic case, the vibration acts not only gravity, but also driving acceleration. Therefore, the actual angles of the acceleration in three dimensions were calculated based on the changed Euler angle of the geometric relationship, as mentioned in equations (1) – (3) (Zhou, et al., 2017). The angle generated from each sensor is susceptible to frequent changes during transportation. Hence, a low-pass filter was added to reduce high fluctuations, as presented in the following equations (4) – (6) to stabilize the acceleration angle. Next, the attitude angle was calculated using complementary filters as expressed in the following equations (7) – (9) to stabilize the rotational angular velocities. Finally, the angle in the radian was converted to degree using equations (10) – (12). Sensors are highly sensitive and require calibration. Thus, this calibration was calculated by subtracting the individual amplitude during operation from the mean amplitude during engine idling, as shown in equation (13). Finally, the power spectrum densities were plotted against the frequency of the signal and dominant frequency of vibration using an existing library in Python. These power spectrum densities were then used for TPA analysis.

$$A_{\phi_{P,i}} = \arctan\sqrt{\frac{A_x}{A_y^2 + A_z^2}} \tag{1}$$

$$A_{\phi_{R,i}} = \arctan\sqrt{\frac{A_y}{A_x^2 + A_z^2}} \tag{2}$$

$$A_{\phi_{Y,i}} = \arctan\sqrt{\frac{A_x^2 + A_y^2}{A_z}} \tag{3}$$

where A_{θ_P}, A_{θ_R}, A_{θ_γ} are the output angles of acceleration, respectively, in the longitudinal axis (A_x), lateral axis (A_y), and vertical axis (A_z) directions.

The angle generated from each sensor is susceptible to frequent changes during transportation. Hence, a low-pass filter was also used to reduce high fluctuations, as presented in the following equations:

$$A_{\theta_{P,i}} = w_1 \times (A_{\theta_{P,i-1}} + A_{x,i} \times \Delta t) + w_2 \times A_{\theta_{P,i}} \tag{4}$$

$$A_{\theta_{R,i}} = w_1 \times (A_{\theta_{R,i-1}} + A_{y,i} \times \Delta t) + w_2 \times A_{\theta_{R,i}} \tag{5}$$

$$A_{\theta_{Y,i}} = w_1 \times (A_{\theta_{Y,i-1}} + A_{z,i} \times \Delta t) + w_2 \times A_{\theta_{Y,i}} \tag{6}$$

$$\theta_{P,i} = w_g \times (\theta_{P,i-1} + G_{x,i} \times \Delta t) + w_a \times A_{\theta_{P,i}} \tag{7}$$

$$\theta_{R,i} = w_g \times (\theta_{R,i-1} + G_{y,i} \times \Delta t) + w_a \times A_{\theta_{R,i}} \tag{8}$$

$$\theta_{Y,i} = w_g \times (\theta_{Y,i-1} + G_{z,i} \times \Delta t) + w_a \times A_{\theta_{Y,i}} \tag{9}$$

where w_1 and w_g is a weight value of 0.95, w_2 and w_a is a weight value of 0.05, i is the individual amplitude, Δt is the time interval. $\theta_{P,i}$, $\theta_{R,i}$, and $\theta_{\gamma,i}$ are the output angles of pitch, roll, and yaw, respectively, in the pitch axis (G_x), roll axis (G_y), and yaw axis (G_z). The time-series data formats in radians were converted into

degrees by default. Then, the actual values of the rotational angular velocity were obtained by multiplying the degree $\theta_{P,i}$, $\theta_{R,i}$, $\theta_{\gamma,i}$ by the individual amplitude, as expressed in equations (10) – (12) below:

$$G_{P,i\_angle} = \cos\left(\theta_{P,i} \times \frac{pi}{180}\right) \tag{10}$$

$$G_{R,i\_angle} = \cos\left(\theta_{R,i} \times \frac{pi}{180}\right) \tag{11}$$

$$G_{Y,i\_angle} = \cos\left(\theta_{Y,i} \times \frac{pi}{180}\right) \tag{12}$$

$$G_{actual} = G_{angle} - G_{idling\_mean} \tag{13}$$

where G_{actual}, G_{angle} and G_{idling_mean} is actual, individual and mean value during engine idling, respectively.

3. 3 Transfer path analysis (TPA)

The TPA principal theorem involves a relationship between the input/reference point signals and the output/response point signal of a block control system. It is generally applied in dynamic cases, whereas in this experiment, a hand tractor moving on an asphalt road was observed. In a dynamic hand tractor, a location at the handgrip was considered as a response point, whereas locations at EF, ER, ET, CH, GB, and MH were regarded as reference points. Yoshida et al. (2018) stated that, for a large structure of mechanical analysis, a large number of reference points and response points are required to be introduced; otherwise, unreliable results would be produced.

Individual elements (PSD) from all the positions obtained from the above calculations were selected for transfer path analysis, as presented in Fig. 4.

Structurally, the PSDs were populated into a 3rd-order tensor $m \times n \times k$, where m is the individual PSD of the engine throttle, n is the individual axis of all reference points, k is the layer of k_{PSD} based on the frequency domain, and Y is the individual axis of the response point (Yoshida et al., 2013).

In other words, the relationship between vector reference point $x(t)$ and vector response point $y(t)$ was calculated typically using a principal component regression method measured in equation (14); therefore, it was simply rewritten as a convolution theorem based on the frequency domain, as in equation (15). $Y(t)$ and $X(f)_i$ are known as elements (PSDs) obtained from the FFT calculation for the response point and reference points, respectively, whereas the unknown parameter $H(f)$ is a transfer function that was measured and analyzed using SVD, as presented in equations (16) – (25) (Nomura, 2011). Then, the transfer function was obtained by the product of the covariance and principal component, which was retrieved from the SVD calculation, as shown in Fig. 5. The importance of TPA with the principal component was to reduce interior noise and unrelated vibration. Finally, the summation of each variance calculated by a polynomial equation is a product of the response point.

The reference point was obtained by repeating the above procedure until the response level satisfied the

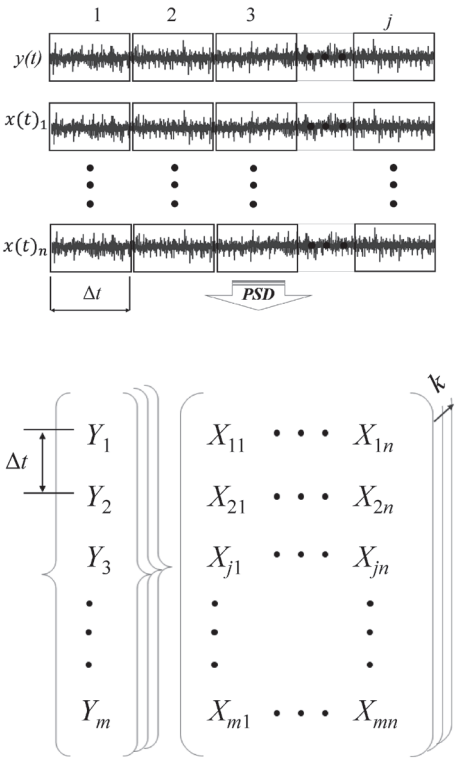

Fig. 4 Data population structure into a three-dimensional tensor flow matrix

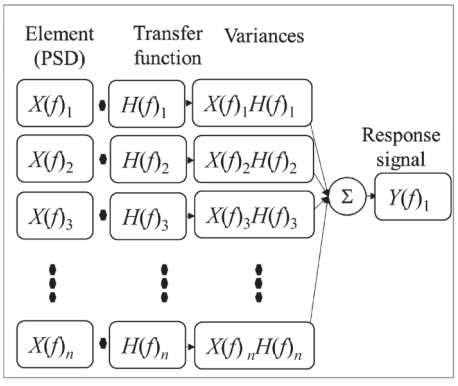

Fig. 5 Diagram of operation of transfer path analysis

target at each frequency (Nomura, 2011). The restructured analysis satisfied the target point based on individual observations. However, in this experiment, a combination of two locations was conducted to obtain the best contribution to the response point. Hence, the best single location derived from this highest combination using root mean square error was concluded.

$$y(t) = \sum_{i=1}^{n} x(t)_i \times h(t)_i \tag{14}$$

$$Y(f) = \sum_{i=1}^{n} X(f)_i . H(f)_i \tag{15}$$

$$\begin{cases} Y(f)_1 = X(f)_{11} H(f)_1 \ldots . + X(f)_{1n} H(f)_n \\ \vdots \\ Y(f)_m = X(f)_{m1} H(f)_1 \ldots . + X(f)_{mn} H(f)_n \end{cases} \tag{16}$$

$$Y(f) = X(f) \times H(f) \tag{17}$$

$$H(f) = [X(f)]^{-1} \times Y(f) \tag{18}$$

$$X(f) = U(f) \times S(f) \times [V(f)]^{-1} \tag{19}$$

$$T(f) = U(f) \times S(f) = X(f) \times V(f) \tag{20}$$

$$Y(f) = T(f) \times C(f) \tag{21}$$

$$C(f) = ([T(f)]^{-1}[T(f)])^{-1} \times [T(f)])^{-1} \times Y(f) \tag{22}$$

$$Y(f) = X(f) \times V(f) \times C(f) \tag{23}$$

$$H(f) = V(f) \times C(f) \tag{24}$$

$$H(f) = V(f) \times [S(f)]^{-1} \times [U(f)]^{-1} \times Y(f) \tag{25}$$

III Results and discussion

1. Results

Reducing the vibration magnitude of a hand tractor is essential for achieving comfortable conditions. During a hand tractor operation, the vibration at the handgrip, which is inevitably held and driven by the operator, should be minimized to an optimum level. However, for a large structural component such as a hand tractor, the vibration elimination process should consider the whole body rather than just the handgrip (Siemens, 2014). The best selected locations with a high contribution to the handgrip can also be achieved satisfactorily.

The TPA technique was used to determine the best and highest contributions. Time series data, which were generated in a complex form from each sensor, consist of unwanted noise and inaccurate data, as presented in Fig. 6, which could lead to a calculation limitation to the use of the TPA method. In the mechanical analysis, the TPA, which is calculated in a time series, has more difficulty to localizing the best reference point with a high contribution; hence, the power spectrum densities obtained by the introduction of FFT at the reference points and the response point were selected and populated into the three-dimensional tensor flow matrix for the TPA analysis. The results confirm that TPA is the best application in the frequency domain (Siemens, 2014).

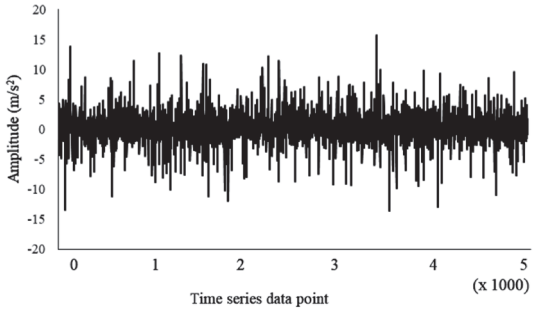

Fig. 6 Time series vibration signal

Analytically, populating the PSD as elements from the reference points and response points into the three-dimensional tensor flow for the TPA calculation, the highest and best contributions at the reference points to the response point were obtained. It can be clearly observed that TPA is a powerful tool for separating noise and actual vibration; thus, it identified the best related contribution and unrelated locations. The application of TPA showed that vibration amplitudes at EF, ER, and ET contributed significantly less to the response point. Fig. 7 (a, b, c, d) presents the results of the vibration contribution from the reference points at EF, ER, and ET to the response point at the handgrip. In addition to the longitudinal, lateral, and vertical axes of the reconstructed analyses, the contribution of the results of the three locations to the response point was marginal, and the important peaks also exhibited visibly small amplitudes at predominant frequencies. At the ER, high peaks emerged at 17, 35, and 17 Hz along the longitudinal, lateral, and vertical axes, where the EF appeared at 52, 35, and 35 Hz, and the ET appeared at 20, 60, and 20 Hz, respectively. These were subsequently compared with those of the acceleration response point at the frequencies of 22, 22, and 22 Hz. Therefore, the locations of ER, EF, and ET were not considered as target points.

However, good variance contributions were observed

at the CH, GB, and MH. Fig. 7 (e, f, g) shows that those variances contributed largely from the reference points at identical predominant frequencies of 22, 22, and 22 Hz at the longitudinal, lateral, and vertical axes to the response point at the highest frequencies of 22, 22, and 22 Hz at the longitudinal, lateral, and vertical axes, respectively. Based on this observation, the locations of the CH, GB, and MH could be set as target points to

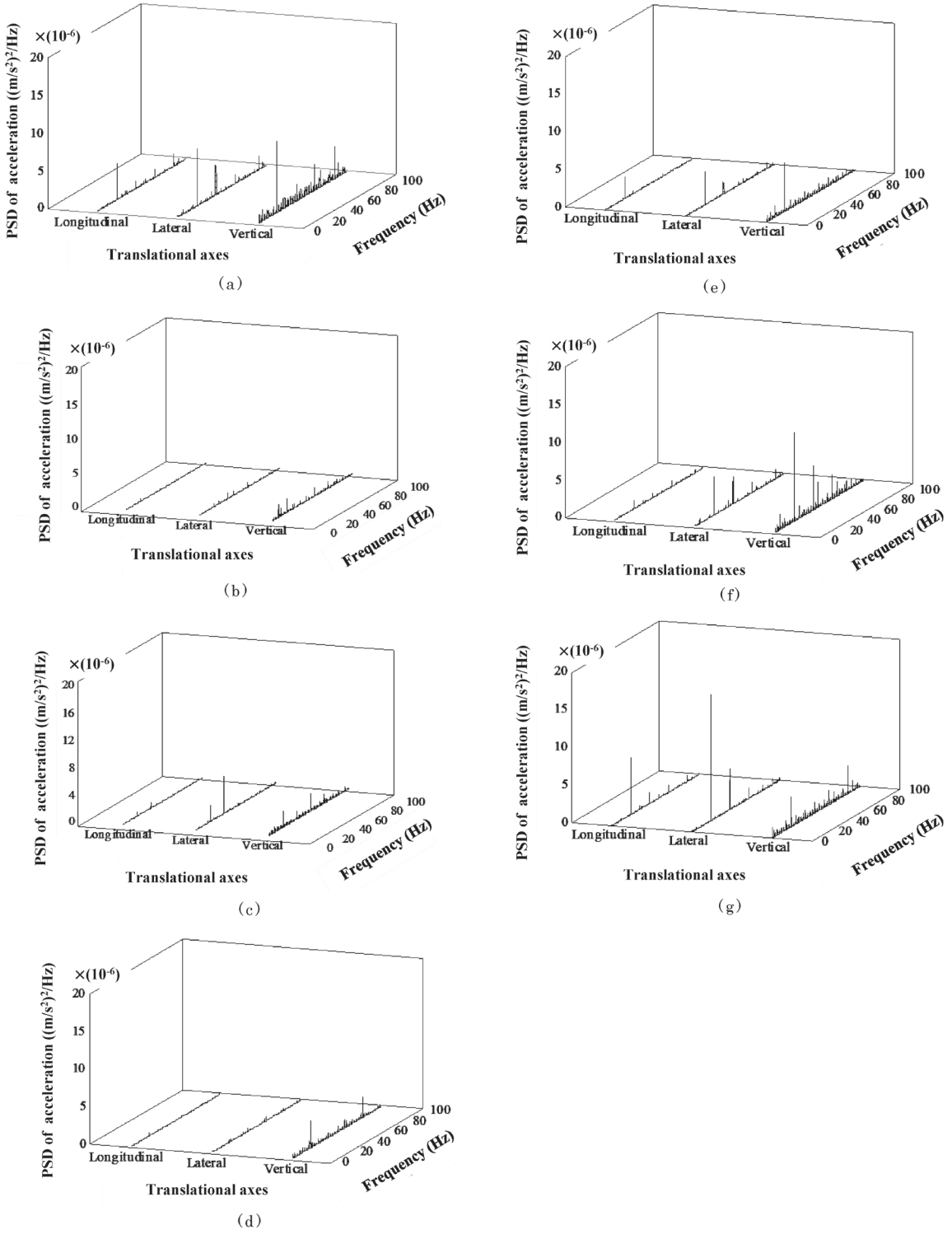

Fig. 7 A comparison of vibration behavior at each reference point using an TPA analytical model to response point at HG: (a) original acceleration data at response point (HG), (b) acceleration reconstruction data at EF, (c) acceleration reconstruction data at ER, (d) acceleration reconstruction data at ET, (e) acceleration reconstruction data at CH, (f) acceleration reconstruction data at GB, (g) acceleration reconstruction data at MH.

the response point of the hand tractor. However, as recommended by Yoshida et al. (2018), for large structures such as vehicle bodies, a combination of multiple locations should be applied to reduce unwanted noise and inaccurate data and enhance the relationship between the input and output. Hence, a combination of two of the three locations was used exclusively.

A combination of two of the three locations was conducted in pairs. These pairs are CH–GB, GB_MH, and CH–MH, provided that these locations involve high-variance contributions to the response point, as described in the aforementioned section. The calculation process of these combinations involved multiplication of the elements of the combination, including all the individual axes and the transfer function. The response point is the sum of the variances, as shown in Fig. 5.

The results showed that, compared to the variances of the combination of GB–MH, the variances of the combination of CH–GB and CH–MH had higher contributions to the response point, as presented in Fig. 8 (a, b, c, d).

The combination of CH–GB, which contributed high variances from the reference to the response point at the predominant frequencies of 22 Hz at all axes, were also found the same tendencies at the combination of CH–MH.

It is definitely understood that the individual variance contributions of these combinations to the response point are large; therefore, these locations could be set as target points for the response point. Nevertheless, it is recommended to consider the best contribution to reduce the number of sensors installed on the hand tractor, and that locations can be used to represent the vibration characteristics at the response point (handgrip). To develop the best reference points with a high contribution to the response point, an inverse time series obtained from an inverse FFT calculation was applied to measure the RMS and RMSE values. The RMS acceleration results are represented in Fig. 9, 10, and 11 for different engine throttles. Good patterns were satisfactorily highlighted alongside various engine throttles at the longitudinal, lateral, and vertical axes between CH–MH, response point signal (response data), and CH–GB.

Considering this, another method, that is, the RMSE

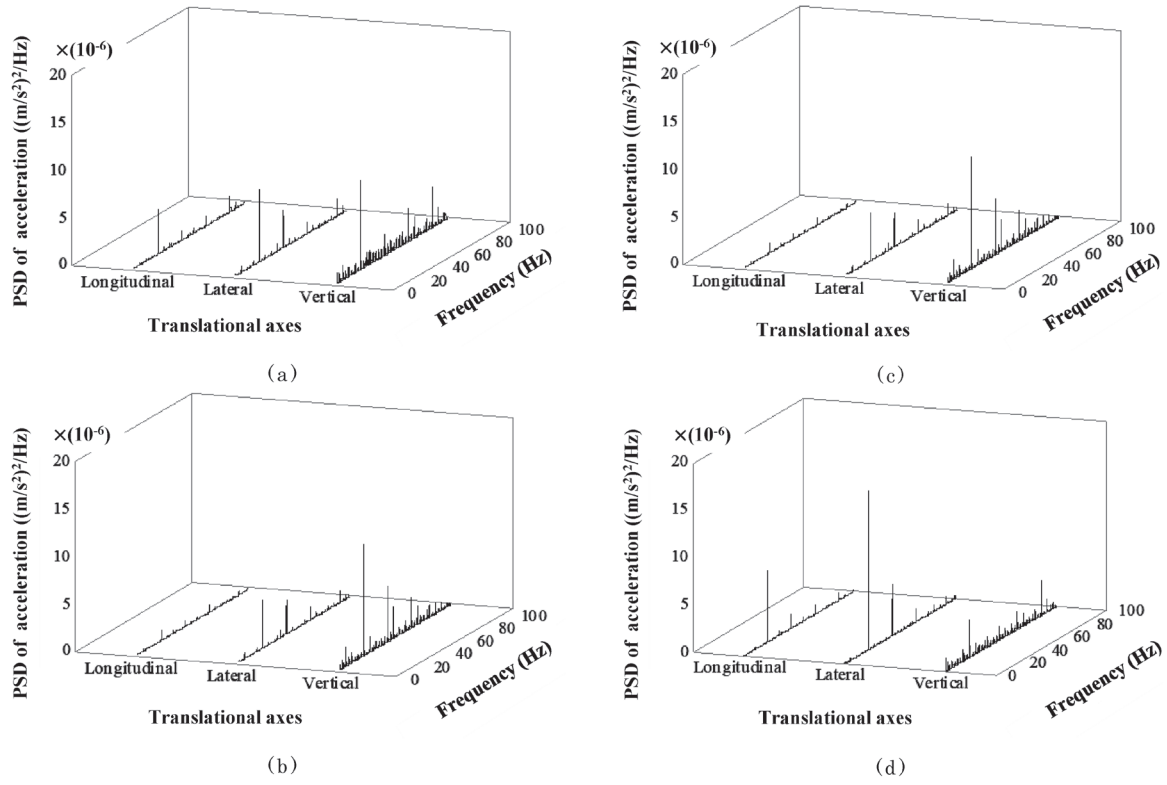

Fig. 8 A comparison of vibration behavior at two combination reference points using an TPA analytical model to response point at HG: (a) original acceleration data at response point (HG), (b) acceleration combination reconstruction points (CH–GB), (c) acceleration combination reconstruction points (GB–MH), (d) acceleration combination reconstruction points (CH–MH).

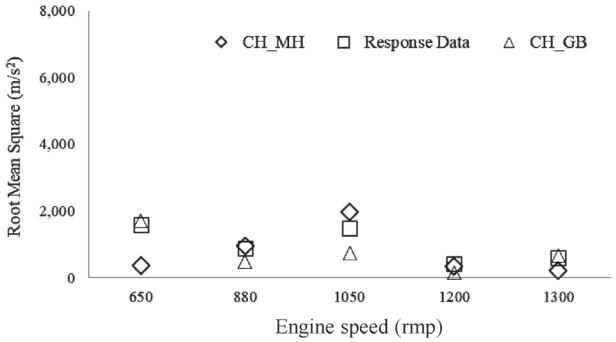

Fig. 9 RMS acceleration of CH–MH, CH–GB and response date at different engine speed along longitudinal axis

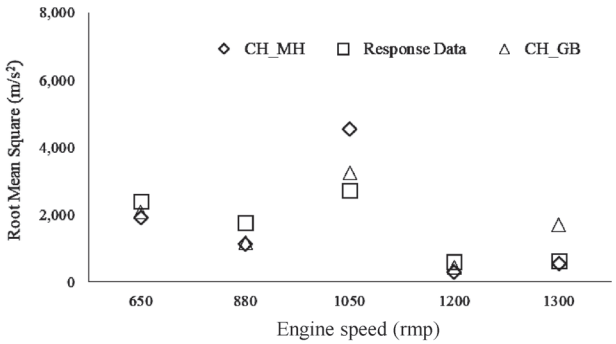

Fig. 10 RMS acceleration of CH–MH, CH–GB and response date at different engine speed along lateral axis

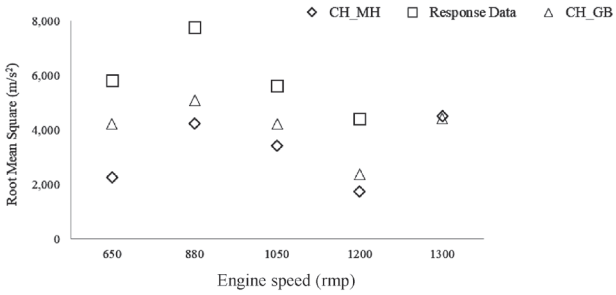

Fig. 11 RMS acceleration of CH–MH, CH–GB and response date at different engine speed along vertical axis

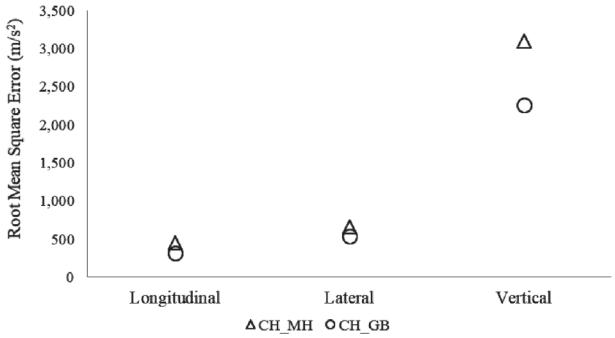

Fig. 12 RMSE acceleration of chassis-mid-handle (CH–MH) and chassis-gearbox (CH–GB) to the response data

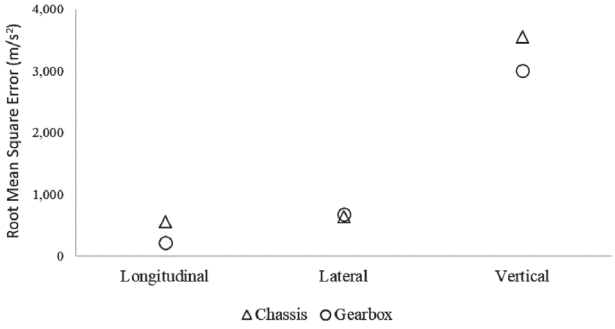

Fig. 13 A comparation of RMSE acceleration between chassis and gearbox to the response data

method, was applied to confirm the result. As shown in Fig. 12, compared to the combination of CH and MH, the combination of CH and GB presented a very low error at all the engine throttles and axes. Hence, the combination of CH and GB is the reference point position that contributes the highest vibration transmission to the response point. Furthermore, in order to investigate the response point with the highest vibration transmission contribution, a comparison of the RMSE acceleration between CH and GB the response data was performed. As a result, the RMSE values at gearbox were lower than those at the chassis. Therefore, it was suggested that the reference point at the gearbox is the best reference point, where represents the highest contribution to the vibration transmission of the handgrip.

2. Discussion

In the experiment, the transfer path analysis technique was used to detect the main contribution of the reference points to the response point of the hand tractor. The power spectrum densities were obtained using the time series data. Siemens (2014) confirmed that transfer path can be applied in the frequency domain. These power spectrum densities were populated into a 3rd-order tensor for the TPA analysis. The technical TPA had high contributions at three reference points of the hand tractor: the chassis, gearbox, and middle between handle-base and handgrip. Yoshida et al. (2013) concluded that TPA performed significantly well in separating the noise and actual vibration, with low and high contributions. Nomura (2011) also mentioned a high contribution from the reconstruction points to the response point when using transfer path analysis. How-

ever, the performance was then evaluated using a combination of two of the three locations, with high contributions, to improve the relationship. Yoshida et al. (2018) recommended that a combination of multiple reference-point signals should be utilized for a large structure, such as a vehicle body; otherwise, inaccurate data would be presented. The first two combinations of the three, CH–GB, CH–GB, and GB–MH, had a higher contribution to the response point. Thus, to obtain the best main contribution, RMS and RMSE were applied. It was concluded that, that the combination of CH–GB contributed highest variances to the response-point signal, and the vibration in the parts between CH and GB, which is middle between the engine and arm sections, has the highest contribution to the vibration reduction at the handgrip. Furthermore, GB is the best target point for the damper. In a dynamic case, vibration may influence from different sources such as road condition and wheel. Chassis and gearbox where are close to wheel are susceptible to external influences. Structurally, chassis and gearbox materials are stiff and highly rigid body that do not absorb vibration well. In reverse, it highly transmits vibration to other connecting parts.

IV Conclusions

In this study, to identify the relationship between the reference points and the response point, seven wireless communication sensors were rigidly taped on different points of the hand tractor, mainly the EF, ER, ET, CH, GB, MH, and HG. The HG was considered as the response point, while the other six locations were regarded as reference points. The TPA technique was used analytically. In the TPA process of this experiment, the power spectrum densities obtained from the calculation of time-series data were manipulated into a 3rd-order tensor for the analysis. This also involved embedding singular value decomposition and multiple linear regression analyses. Finally, the relationship between the reference points and the response point was obtained using a polynomial equation in the reduction loop. The calculations were manually programmed using Python.

The results showed that TPA performed significantly well in separating the unwanted signal and noise and identifying the best target reference points to the response point. For individual location performance with TPA, high contributions were found at CH, GB, and MH; however, low relationships were found at EF, ER, and ET. A combination of two of the three locations, which are CH–GB, GB–MH, and CH–MH, contributed significantly to improving the abovementioned relationship. The results showed that the combinations of CH–GB and CH–MH showed a higher contribution to the response point than the combination of GB–MH. To obtain the best reference points, the root mean square and root mean square errors from the inverse FFT were used. The results showed that the CH–GB combination contributed strongly to the response point. Therefore, the locations, CH, and GB can be used in a compound set as the target point. Thus, to determine the improvement part to reduce the vibration of the handgrip, the most affected reference point was studied. Result presented that the location at GB is the best reference point, hence, this location can be used as a vibration damper instead of handgrip.

Acknowledgments

This work was supported by JSPS KAKENHI (grant number JP20K06323).

References

Chan S., 2013. Cambodia perspective on rice production and mechanization in Cambodia. Department of Agricultural Engineering, 1–29.

Cowell, P.A., 1969. Automatic control of tractor mounted implements-an implement transfer function analyser. Journal of Agricultural Engineering Research, 14 (2), 117–125.

Dewangan, K.N., Tewari. V.K., 2008. Characteristics of vibration transmission in the hand-arm system and subjective response during field operation of a hand tractor. Biosystems Engineering, 100, 535–546.

Erdal, K., Erkan, K., Herman, R., Wouter, S., 2013. Modeling and identification of the yaw dynamics of an autonomous tractor. 9th Asian Control Conference (ASCC) 2013, 1(6).

FAO, 2013. Mechanization for rural development: a review of patterns and progress from around the world. Integrated Crop Management, 20–2013.

Nomura, K., Yoshida, J., 2006. Method of transfer path analysis for vehicle interior sound with no excitation experiment. F2006D183, Proceedings of FISITA World Automotive Congress, Yokohama, Japan.

Nomura, K., 2011. Theory and example of operational transfer path analysis. Acoustical Science and Technology, 67(4), 163–168.

Salokhe, V. M., Majumdar, B., Islam, M. S., 1995. Vibration characteristics of a power tiller. Journal of Terramechanics, 32(4), 181–197.

Sam, B., Kathirvel. K., 2006. Vibration characteristics of walking and riding type power tillers. Biosystems Engineering, 95(4), 517–528.

Siemens PLM Software, 2014. Advanced transfer path analysis techniques.

Singh T.V., Kumar R.M., Viraktamath. B.C., 2011. Selective mechanization in rice cultivation for energy saving and enhancing profitability. Rice Knowledge Management Portal (RKMP), India.

Tiwari, P.S., Gite, L.P., 2006. Evaluation of work-rest schedules during operation of a rotary power tiller. International Journal of Industrial Ergonomics, 36, 203–210.

Yoshida, J., Yamashita, D., 2013. Target level setting method for the reference signal of operational TPA. Journal of

System Design and Dynamics, 7(4), 317–327.
Yoshida, J., Majima, R., Isemura, J., 2018. Obtaining method of high contributing whole body principal component mode by separated measurements. Mechanical Engineering Letters, 4, 18–00290.
Zhou, Y., Cui, S., Wang, Y., Zhai, L., 2017. A refined attitude algorithm for AUV based on IMU. In Proceedings of the International Conference on Scientific Computing (CSC), 16–22.
（Received：15. September. 2022・Accepted：15. February. 2023・Question time limit：31. July. 2023）

［技術論文］

伝達経路解析に基づく歩行式トラクタの目標振動予測のための参照点の検出法

プン ソヴァタナ*1・井上英二*2・光岡宗司*3†・岡安崇史*2・平井康丸*2

要　旨

本研究では，伝達経路分析 (TPA) により，歩行式トラクタの応答点振動に対する最適な参照点の推定を試みた。エンジン右側の前後，エンジン上部，シャーシ，ギアボックス, アーム中央の 6 箇所を参照点, ハンドグリップを応答点とした。TPA 分析では，参照点と応答点のパワースペクトル密度の 3 階テンソルデータを用いて解析を行った。応答点振動の推定精度を向上させるため，6 つの参照点から 2 つを選び TPA 解析を行った。参照点信号から推定された応答点振動の二乗平均平方根誤差より、最も寄与度の高い参照点の組を決定した。その結果，応答点の振動の推定に最適な参照点は、シャーシとギアボックスの組み合わせであることが示された。

［キーワード］伝達経路解析，振動特性，ハンドトラクタ，参照信号，目標信号

＊1 会員　カンボジア王国農林水産省プーサ州農林水産部門
＊2 会員　九州大学大学院農学研究院（〒812–0395 福岡市西区元岡 744　Tel 092–802–4635）
*3 会員　琉球大学農学部（〒903–0213 沖縄県西原町千原 1 番地 Tel 098–895–8768）
† Corresponding author : mitsuoka@agr.u-ryukyu.ac.jp.